Iron(I) Tetraphenylporphyrin is an Active Catalyst in Reductive Deoxygenation when Switching from CO_2 to Isoelectronic N_2O

Camille Chartier, Rana Deeba, Alexandra Collard, Sylvie Chardon-Noblat, Cyrille Costentin

Iron(I) Tetraphenylporphyrin is an Active Catalyst in Reductive Deoxygenation when Switching from CO_2 to Isoelectronic N_2O.

Camille Chartier, Rana Deeba, Alexandra Collard, Sylvie Chardon-Noblat and Cyrille Costentin*

Univ Grenoble Alpes, DCM, CNRS, 38000 Grenoble, France.

Keywords: Nitrous oxide, Reductive deoxygenation, Electrochemistry, Molecular catalysis, Carbon dioxide

ABSTRACT: The electrochemical reductive deoxygenation of N_2O catalyzed by the iron tetraphenylporphyrin (TPPFe) is studied and compared to the electroreduction of CO_2 to CO by the same catalyst. We show that the electroreduction of N_2O is catalyzed by TPPFe(I) albeit at a slower rate compared to TPPFe(0). On a similar timescale, CO_2 does not react with TPPFe(I). The catalytic reduction of N_2O by TPPFe(I) is however endowed by a self-modulation process due to the production of hydroxide ions as co-product, that bind to TPPFe(II) and slow down the regeneration of the TPPFe(I) catalytic active species. Two catalytic cycles are thus intertwined when the electrocatalysis is run at a potential where TPPFe(0) is generated, and the resting state in solution is TPPFe(II)(OH) and not TPPFe(I), as opposed to the case of CO_2 catalytic reductive deoxygenation. Revealing the shift of the active catalysis from TPPFe(0) to TPPFe(I) opens the way toward the design of molecular catalysts for N_2O reductive deoxygenation at lower overpotential.

Introduction

Activation of small molecules is a field of intense research activity because it may be involved in energy storage processes. [1] CO_2 conversion to CO is one of the most salient examples with numerous contributions devoted to understand catalytic processes at work in the corresponding electroreduction, whether it involves molecular catalysts [2] or heterogeneous electrocatalysts. [3] Besides energy storage, small molecules activation is also important in biological systems such as those involved in the nitrogen cycle where the denitrification pathway consists of a chain of individual steps carried out by separate enzymes, beginning with nitrite reductase to nitric oxide reductase, and ending with nitrous oxide reductase to release nitrogen gas. [4] Nitrous oxide (N_2O) reduction to N_2 is not only important to prevent accumulation of this greenhouse gas in the atmosphere, but it is also interesting because, due to the stability of the N_2 product formed, N_2O is potentially a strong oxidant with numerous examples of its use as such already reported. [5] However, oxidation of substrates (S_{red}) by N_2O requires catalysis (Cat) because of its kinetic inertness (Scheme 1). Decoupling N_2O reductive activation and the substrate oxidation as sketched at the bottom of scheme 1 allows focusing on the mechanistic understanding of N_2O reductive deoxygenation. In that regard, molecular catalysis of N_2O electroreduction is an attractive approach and, recently, we have shown that the well-studied [Re(bpy)(CO)$_3$Cl] catalyst for CO_2 to CO conversion is actually a competent catalyst for N_2O electroreduction. [6] N_2O and CO_2 are isoelectronic molecules with both an electrophilic central atom, it is therefore appealing to consider that they may have similar reactivity toward low valent transition metal complexes. Another well-studied catalyst for CO_2 to CO conversion, iron tetraphenylporphyrin (TPPFe), [7] was indeed also shown to be an efficient catalyst for N_2O reduction provided the formal TPPFe(0) redox state is generated. [8] However, it has been previously reported that a Fe(I) porphyrin could reduce N_2O and generate Fe(III) porphyrin. [9] Hemic myoglobin immobilized on electrodes has also been reported to catalyze N_2O reduction in water at the level of the Fe(II)/Fe(I) redox couple. [10] This prompted us to investigate the reactivity of TPPFe with N_2O. In that endeavor, and from a mechanistic point of view, N_2O reactivity comparison with CO_2 isoelectronic molecule is of potent interest. TPPFe(0) is a well-known reductant for CO_2 but the Fe(I) formal state in TPPFe does not reduce CO_2. However, the reactivity of Fe(I) can be turned on provided an appropriate modification of the porphyrin ligand environment is designed. [11,12] These results also resonate with the finding that Fe(I) state of iron porphyrinoid can activate CO_2 for its conversion to HCOOH. [13]

Scheme 1. Principle of N_2O reductive deoxygenation (E^{2+} and E'^{2+} = electrophiles, S_{red} = chemical reductant)

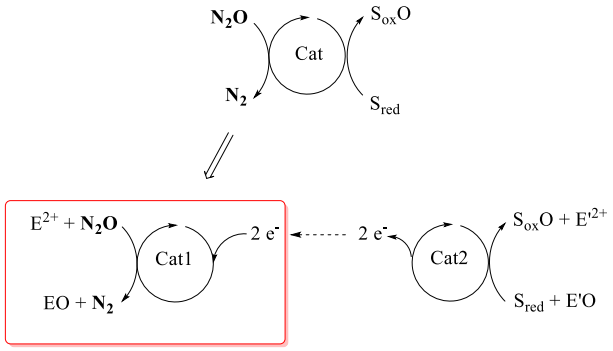

Herein, we thus investigate in detail the electroreduction of N_2O in dimethylformamide (DMF) catalyzed by TPPFe and we show that TPPFe(I) is a competent reductant albeit at a slower rate compared to TPPFe(0) and despite being endowed by a self-modulation process. An overall mechanism with two intertwined catalytic cycles is revealed showing a different behavior of both isoelectronic N_2O and CO_2 molecules to be activated. Beyond resolving molecule activation mechanisms these results allow to open new directions on the way to decrease the overpotential of reductive deoxygenation reactions.

Results and Discussion

Cyclic voltammetry analysis

Cyclic voltammetry (CV) of TPPFe(Cl) in DMF under argon exhibits three reversible waves assigned to the formal Fe(III)/Fe(II), Fe(II)/Fe(I) and Fe(I)/Fe(0) redox couples. The first wave is coupled with a chloro ligand exchange with DMF. Its reoxidation is therefore split in two contributions as previously detailed (Figure 1a). [14] As already established, under an atmosphere of N_2O or CO_2, a catalytic wave develops at the level of the formal Fe(I)/Fe(0) redox couple (Figure 1a and 1b).[7,8] Note that, here, no addition of a proton donor was made; the proton source is the residual water present in DMF electrolyte solution.

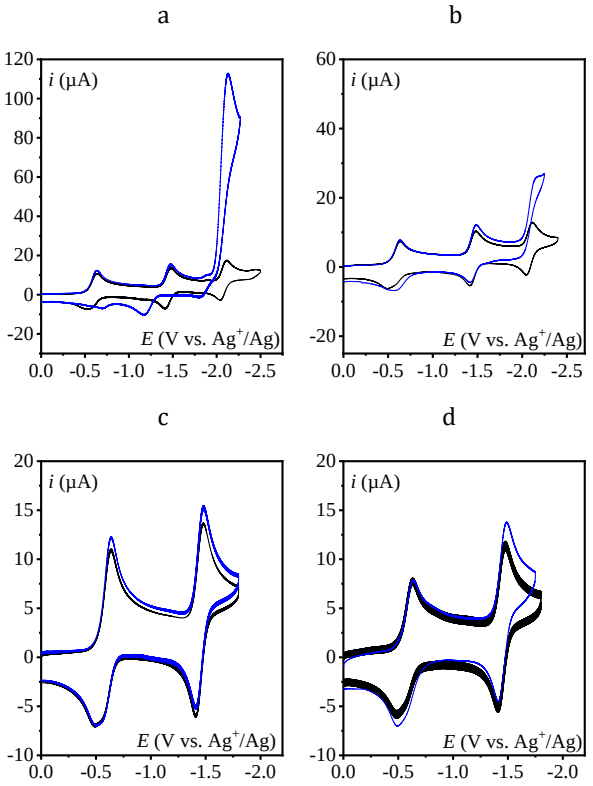

Figure 1. CVs in DMF + 0.1 M *n*-Bu_4NPF_6 at 0.1 V/s on a 3 mm diameter GCE. (a) and (c) TPPFeCl (1 mM) under argon (black) and under N_2O (blue). (b) and (d) TPPFeCl (0.7 mM) under argon (black) and under CO_2 (blue).

No significant increase of the current is observed at the level of the Fe(II)/Fe(I) redox couple. This observation indicates that, on the timescale of the CV, there is no irreversible reaction between TPPFe(I) and N_2O or CO_2. Therefore, a pseudo-first order rate constant for reaction between TPPFe(I) and CO_2 or N_2O would be less than 0.05 s^{-1} (see Supporting Information (SI) for details). Additionally, no shift of the Fe(II)/Fe(I) waves is observed (Figures 1c and 1d). It indicates that, if N_2O and/or CO_2 interact reversibly with TPPFe(I), it is a weak interaction with an association constant being smaller than 4 M^{-1} (see SI for details), as also observed under CO_2 in acetonitrile. [15] Consequently, it makes at equilibrium the adduct between TPPFe(I) and CO_2 or N_2O, if any, a minority species. [16] Another important observation on the CVs is that the reoxidation waves are at very different positions in the presence of N_2O compared to CO_2 (Figures 1a and b respectively), suggesting that the resting state is different in both cases. Altogether, this survey of the CVs of TPPFe(Cl) in the presence of N_2O and CO_2 confirms that TPPFe(0) is a competent reductant for both N_2O and CO_2 but mechanistic details might be different. It also indicates that neither CO_2 nor N_2O are reduced by TPPFe(I) in organic solvent on the timescale of the CV and none of these two substrates forms a thermodynamically favorable adduct with TPPFe(I) in the concentration range of millimolar.

TPPFe(0) as an active catalyst

To get insights into the reactivity of TPPFe(0) with N_2O, a solution of TPPFe(0) was prepared via a three-electron exhaustive electrolysis of TPPFe(III)(PF_6). Hence, a constant potential corresponding to -2.20 V vs. Ag^+/Ag (all potentials are referred to this reference electrode throughout the paper; see SI to report the potential vs. SCE) was applied to a 0.5 mM TPPFe(III)(PF_6) in DMF + 0.1 M KPF_6. KPF_6 electrolyte was used instead of *n*-Bu_4NPF_6 to prevent any possible reactivity of TPPFe(0) with *n*-Bu_4N^+. [17] It should be noted that the alkylation of TPPFe(0) with *n*-Bu_4N^+ does not occur on the timescale of the CV as attested by the chemical reversibility of the Fe(0)/Fe(I) redox couple (Figure 1, black CVs), For the same reason, on the timescale of the CV, nor does occur the formation of a phlorin via protonation of the ring of TPPFe(0) by residual water as recently shown for a Fe(0) porphyrin with trimethylammonium substituents. [18] Alkylation with *n*-Bu_4N^+ can take place on longer timescale and thus decreases the amount of TPPFe(0) if electrolysis is run in *n*-Bu_4NPF_6 as supporting electrolyte. [19] The use of KPF_6, as supporting electrolyte, also requires to get rid of the chloro ligand of TPPFe(Cl) to prevent KCl precipitation in DMF upon reduction. Hence, from now on, TPPFe(PF_6) synthesized from TPPFe(Cl) (see SI) is used as the starting material. Monitoring the constant potential electrolysis by UV-vis (Figure 2b) shows the successive conversion of TPPFe(III) to TPPFe(II), then to TPPFe(I) and finally to TPPFe(0). The characteristic absorption Q-bands of the different species are gathered in Table S1. Moreover, the formation of TPPFe(0) is attested by its characteristic Soret bands at 360 and 460 nm (figure S3; see also in SI a detail of all observations unambiguously showing formation of TPPFe(0)). [20,21]

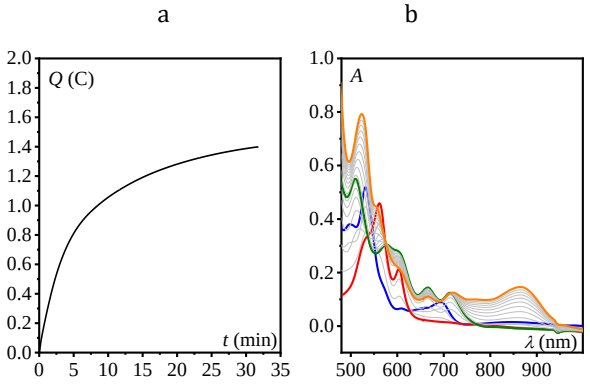

Figure 2. (a) Charge passed vs. time. (b) In situ time evolution of UV-vis spectra (*l* = 1 mm, 1 scan / 50 s). Initial spectrum in blue (TPPFe(III)), spectrum after 0.5 C in red (TPPFe(II)), after 1 C in green (TPPFe(I)), after 1.45 C in orange (TPPFe(0)) during exhaustive controlled potential electrolysis at -2.20 V of TPPFe(III)(PF_6) (0.5 mM) in DMF + 0.1 M KPF_6 (V = 10 mL)

on a carbon felt electrode under argon.

In the presence of N_2O (14 mM, see SI for details on the protocol for addition of N_2O), the electrogenerated 0.5 mM solution of TPPFe(0) shows a rapid decrease of the absorbance at 864 nm indicating a fast reaction with quasi quantitative consumption of TPPFe(0) in less than 10 seconds (Figures 3a and b). Control experiments of the stability of TPPFe(0) by addition of DMF on TPPFe(0) electrolyte solution demonstrate that the disappearance of TPPFe(0), on this time scale, is due to N_2O and not to any residual source of protons or oxygen present in the solvent (Figure S4). Similarly, addition of CO_2 (11 mM) to an electrogenerated 0.5 mM solution of TPPFe(0) shows a reaction with TPPFe(0). Both are consistent with the observation of a catalytic wave in CV at the level of the TPPFe(I)/TPPFe(0) couple under N_2O or CO_2 atmosphere (Figures 1a and b). In the case of the addition of CO_2, UV-vis data indicates that TPPFe(0) is converted into TPPFe(I) without further evolution. This is consistent with the proposed mechanism for CO_2 reduction by TPPFe(0) where TPPFe(0) reduces CO_2 by two electrons to form TPPFe(II)(CO) which does not accumulate because it is immediately reduced by a second TPPFe(0) molecule. [7] The absence of further evolution of TPPFe(I) despite CO_2 being in excess clearly shows that TPPFe(I) is not able to reduce CO_2, at least on the timescale of 10 min.

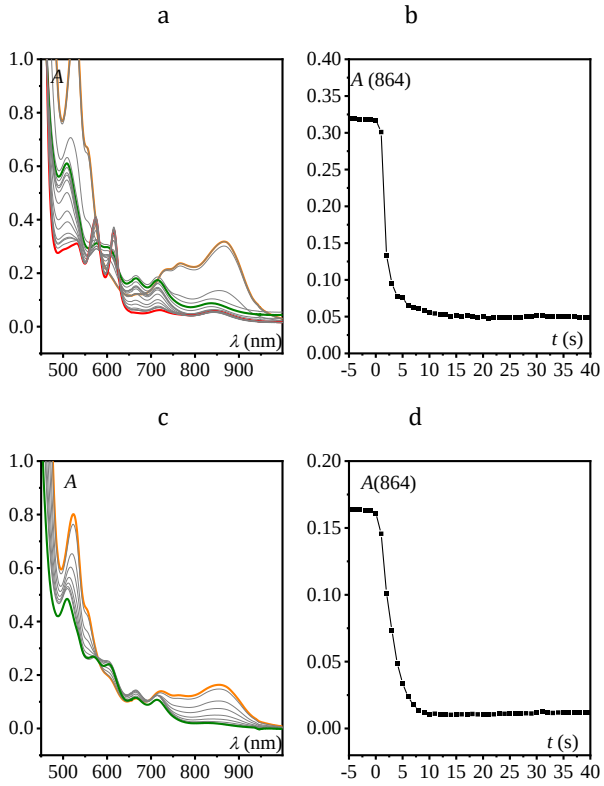

Figure 3. (a) Time evolution of UV-vis spectra (l = 1 mm, 1 scan / 1 s) of a 0.5 mM solution of electrogenerated TPPFe(0) in DMF + 0.1 M KPF_6 with N_2O leading to a concentration of 14 mM. Initial spectrum in orange at t = 0 (addition); intermediate spectrum in green after 52 s, spectrum in red after 600 s. (b) Time evolution of the absorbance at 864 nm characteristic of TPPFe(0) absorption. (c) Time evolution of UV-vis spectra (l = 1 mm, 1 scan / 1 s) of a 0.5 mM solution of electrogenerated TPPFe(0) in DMF + 0.1 M KPF_6 with the addition of CO_2 leading to a concentration of 11 mM. Initial spectrum in orange at t = 0 (addition), final spectrum in green. (d) Time evolution of the absorbance at 864 nm characteristic of TPPFe(0) absorption.

TPPFe(I) as an active catalyst

In the case of the addition of N_2O, TPPFe(0) is quickly converted to TPPFe(I) (in less than 10 seconds) as identified by its UV-vis spectrum (Q-bands at 510, 575, 605, 664, 714 nm, seeTable S1 and Figure 3a, green curve; see also Figure S5), but then, on a longer timescale (≈ 10 min), the UV-vis spectrum changes and TPPFe(I) is converted to a new species with UV-vis Q-band features at 574 and 616 nm, hence corresponding to those of a species identified as TPPFe(II)(OH) (Table S1). Monitoring the absorbance at 575 nm, where the molar extinction coefficient of TPPFe(0) is larger than the one of TPPFe(I), we clearly observe upon addition of N_2O, a first rapid decrease of the absorbance (within 10 s) and then an increase of the absorbance on a timescale corresponding to hundreds of seconds (Figure 4). We thus propose that there is an initial fast reduction of N_2O by TPPFe(0) leading to TPPFe(I) according to a reaction sequence that could be akin to the reduction of CO_2 reduction as shown in Scheme 2.

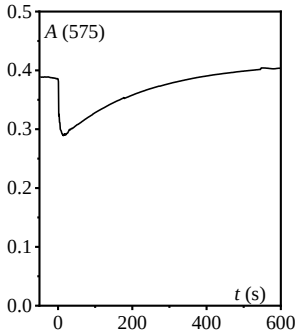

Figure 4. Time evolution of the absorbance at 574 nm (l = 1 mm, 1 scan / 1 s) of a 0.5 mM solution of electrogenerated TPPFe(0) in DMF + 0.1 M KPF_6 (t < 0 s) and in the presence of 14 mM of N_2O.

Scheme 2. N_2O reduction by TPPFe(0)

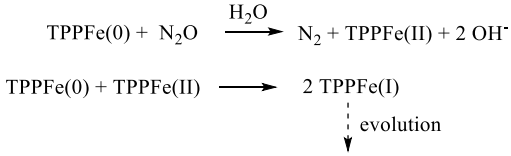

Importantly, the second process, that takes place on longer timescale, can be attributed to the reduction of N_2O by TPPFe(I). As already mentioned, such a reaction does not occur on the timescale of CV but it can be observed on longer timescale. To confirm such a reactivity, a 0.5 mM solution of TPPFe(I) was prepared by an exhaustive electrolysis of TPPFe(III)(PF_6) at -1.80 V (Figure S6) and then N_2O (7 mM) was added. Upon addition of N_2O, TPPFe(I) is converted to TPPFe(II) as attested by UV-vis spectroscopy (Figure 5). The final UV-vis spectrum shows the characteristic Q-band features of TPPFe(II). Isosbestic points are observed at 546, 580, 620 and 621 nm in the Q-bands region. It clearly indicates that no intermediate species accumulate in the course of the

reaction. Getting mechanistic information therefore relies on a kinetic study. The decay of TPPFe(I) is monitored by following the time evolution of the absorbance at 714 nm (Figure 5b) confirming a much slower reaction with N_2O than the one observed in the case of TPPFe(0).

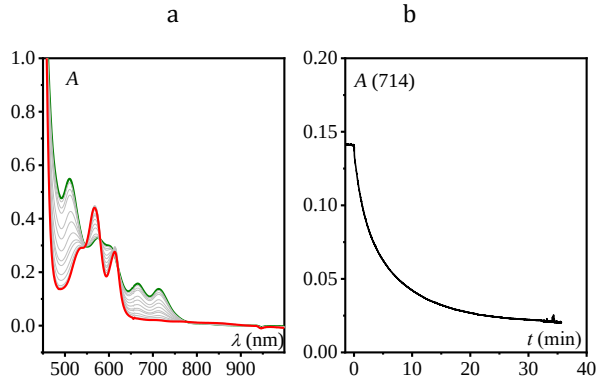

Figure 5. (a) Time evolution of UV-vis spectra (l = 1 mm, 1 scan / 1 s; not all spectra shown) of a 0.5 mM solution of electrogenerated TPPFe(I) in DMF + 0.1 M KPF_6 with the addition of 7 mM of N_2O. Initial spectrum in green at t = 0 (addition), final spectrum in red. (b) Time evolution of the absorbance at 714 nm characteristic of TPPFe(I) absorption.

Reduction of N_2O to N_2 catalyzed by TPPFe(I) was confirmed by running a constant potential electrolysis at -1.80 V in the presence of 0.5 mM TPPFe(III)(PF_6) under an atmosphere of N_2O (Figure S7). Analysis of the head-space gas by GC shows that N_2 was produced with a faradaic yield of 75% (see SI for details).

To gain some insights into the mechanism, the homogeneous reduction of N_2O by electrogenerated TPPFe(I) was monitored by UV-vis spectroscopy at various concentrations of N_2O. Decay of the absorbance at 714 nm allows to follow the time evolution of TPPFe(I). As shown in figure 6a, TPPFe(I) concentration follows, at least at the shorter time, a second order decay according to equation (1):

$$\frac{[\mathrm{TPPFe(I)}]_{t=0}}{[\mathrm{TPPFe(I)}]} - 1 = k_{ap}[\mathrm{TPPFe(I)}]_{t=0}\, t \qquad (1)$$

The apparent rate constant k_{ap} increases with the concentration of N_2O. Because the precise concentration of N_2O is not easy to control in our protocol (see SI for details), the reaction order for N_2O cannot be accurately evaluated from these experiments. However, considering a first order reaction in N_2O seems to be reasonable (Figure 6b). Therefore, based on these kinetic results, second order in TPPFe(I) and first order in N_2O, we can unequivocally conclude that the rate determining sequence involves a two steps mechanism with an intermediate being at steady-state and therefore not spectroscopically detectable. Lowering the temperature would not necessarily make its steady-state concentration larger, nor would it guarantee that the mechanism remains the same. Several mechanisms can be envisioned. A dismutation of TPPFe(I) generating a low concentration of TPPFe(0) that would reduce N_2O. As shown in the SI, such a mechanism can be ruled out based on rate constants evaluation. We are thus left with a process involving first, an equilibrated uphill reaction between TPPFe(I) and N_2O followed by an irreversible step involving TPPFe(I) as depicted in scheme 3. (see SI for details on the establishment of the kinetic law). The proposed mechanism corresponds to an innersphere reduction of N_2O by TPPFe(I). As already pointed out, the intermediate cannot be characterized due to its transient nature. Finally, we emphasize that a purely outersphere process leading to N_2O radical anion as an intermediate can be ruled out from kinetic consideration (see SI).

Scheme 3. N_2O reduction by TPPFe(0)

$$\mathrm{TPPFe(I)} + N_2O \rightleftharpoons \{\mathrm{TPPFe(I)}...N_2O\}$$

$$\mathrm{TPPFe(I)} + \{\mathrm{TPPFe(I)}...N_2O\} \xrightarrow{H_2O} N_2 + 2\ \mathrm{TPPFe(II)} + 2\ OH^-$$

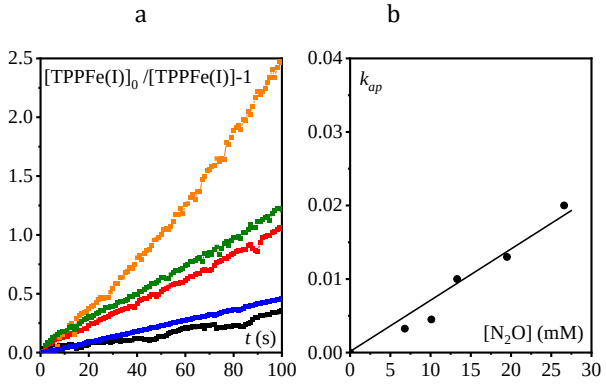

Figure 6. (a) Time evolution of the inverse of the concentration of TPPFe(I) (initially 0.5 mM) in DMF + 0.1 M KPF_6 in the presence of N_2O: 6.8 (black), 10.1 (blue), 13.3 (red), 19.5 (green), 26.5 (orange) mM. (b) Apparent rate constant k_{ap} as a function of N_2O concentration, according to equation (1).

Self-modulation and intertwined mechanisms

We have recently shown that OH^- binds TPPFe(II) with an association equilibrium constant in DMF + 0.1 M KPF_6 equal to 630 M^{-1}.[22] Therefore, we anticipate that, if hydroxide ions are indeed produced upon reduction of N_2O to N_2 as indicated in Scheme 3, a maximal fraction of 20% of the final TPPFe(II) would be under the form of TPPFe(II)(OH) considering the initial 0.5 mM of TPPFe(I). It is in line with the UV-vis spectrum obtained few minutes after addition of N_2O to 0.5 mM TPPFe(I) with Q-bands corresponding to TPPFe(II) (535(sh), 562, 604 nm, Table S1). Alternatively, the UV-vis spectrum obtained few minutes after addition of N_2O to 0.5 mM TPPFe(0) is slightly different and corresponds to a larger fraction of TPPFe(II)(OH) presumably because two equivalents of hydroxide may have been produced corresponding to the successive reduction of N_2O by TPPFe(0) and TPPFe(I) (Figure S8).

If we now consider the electrochemical reduction of N_2O homogeneously catalyzed by TPPFe(I), due to the production of hydroxide ions during catalysis, the actual catalyst is expected to shift from the TPPFe(II)/TPPFe(I) redox couple to the TPPFe(II)(OH)/TPPFe(I) redox couple noting that the binding constant of OH^- with TPPFe(I) is only 1.5 10^{-3} M^{-1}.[22] We thus performed a constant potential electrolysis at -1.80 V under a flux of N_2O in the presence of TPPFe(III)(PF_6) 0.5

mM in solution while monitoring the UV-vis spectrum of the bulk solution (Figure 7a-d). The initial UV-vis spectrum of TPPFe(III)(PF_6) rapidly changes to the UV-vis spectrum of TPPFe(II) (in 2.5 min) after the passage of one mole of electron per mole of Fe complex (0.5 C). Then, catalysis starts and TPPFe(II) is progressively transformed into TPPFe(II)(OH), between t = 2.5 min and 11 min (Figure 7c-d). During this period, the electrolysis current decreases and then it stabilizes at ca. 1 mA (Figure 7a). Once the current is stable, the resting state in solution remains TPPFe(II)(OH). Note that all the useful spectroelectrochemical data regarding TPPFe(OH) are detailed in reference 22.

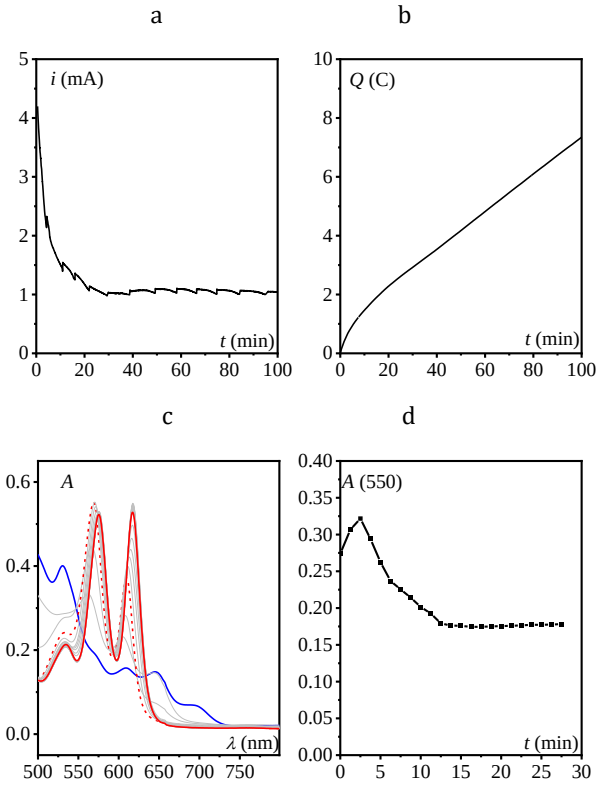

Figure 7. (a) Current over time upon electrolysis at -1.80 V of TPPFe(III)(PF_6) (0.5 mM) in 10 mL of DMF + 0.1 M KPF_6 under N_2O (b) Charge consumed over time. (c) Time evolution of UV-vis spectra (l = 1 mm, 1 scan / 75 s). Initial spectrum (TPPFe(III)) in blue, spectrum after 3.25 min in dashed red, final spectrum in red after 29 min. (d) Time evolution of the absorbance at 550 nm.

The transformation of the resting state in the bulk of the solution can be visualized by following the time evolution of the absorbance at 550 nm (Figure 7d) which initially increases due to the complete conversion of TPPFe(III) to TPPFe(II) and then decreases upon transformation of TPPFe(II) to TPPFe(II)(OH). The decrease of the catalytic current concomitant with the transformation of TPPFe(II) to TPPFe(II)(OH) in the bulk (Figures 7a and c) can be explained by the cathodic shift of the Fe(II)/Fe(I) redox couple with increasing amount of hydroxide. [22] With excess of hydroxide ions, the reduction of TPPFe(II)(OH) to produce the active form of the catalyst TPPFe(I) indeed occurs at more reducing potential, ca. -1.77 V (Figure S9). Therefore, performing the electrolysis at -1.80 V does not allow to get the maximal current density because only a fraction of the active catalyst is formed in the diffusion-reaction layer. [23] A similar electrolysis was also run at -1.65 V, a potential at which TPPFe(II)(OH) is not directly reduced. It shows again a transformation of TPPFe(II) to TPPFe(II)(OH) in the bulk of the solution and a slowing down of catalysis (Figure S10). The catalytic current is then probably limited by a CE process corresponding to the slow dissociation chemical reaction (C) of TPPFe(II)(OH) into TPPFe(II) and OH^- for which the rate constant has been previously estimated to be 0.04 s^{-1}.[22] The mechanism is summarized in Scheme 4. It corresponds to a self-modulation of catalysis as previously anticipated. [22] The same phenomenon was also observed in the case of the electrochemical reduction of N_2O catalyzed by a rhenium triscarbonyl bipyridyl complex. [24]

Scheme 4. Electrochemical reduction of N_2O catalyzed by TPPFe(I)

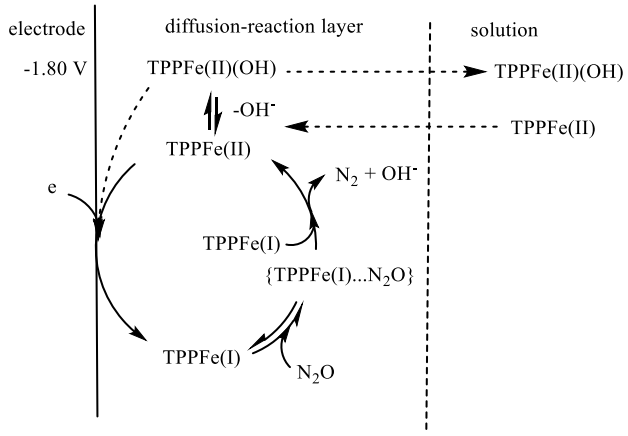

During electrolysis initially run at -1.80 V, after 100 min and the passage of 7 C (Figure 7), the potential was switched to -2.20 V, a potential at which catalysis of N_2O reduction with TPPFe(0) active catalyst is triggered. The catalytic current increases from 1 mA (Figure 7a) to 3 mA (Figure 8a). It then steadily decreases, presumably because the source of protons (most likely water present in the solvent and in the supporting electrolyte) decreases and cannot sustain the catalytic current. Nonetheless, the resting state in solution remains unchanged and corresponds to TPPFe(II)(OH) (Figure 8b). Of note, this resting state corresponds to the previously reported unidentified species as being the product of the reaction between N_2O and TPPFe(0) and the resting state under catalytic conditions. [8] Based on the catalytic CV (Figure 1a), it could have been expected that the resting state in solution would be TPPFe(I), as observed in the case of CO_2 electroreduction catalyzed by TPPFe at -2.10 V. [19] However, as shown above, TPPFe(I) itself catalyzes the reduction of N_2O and therefore the resting state in solution is TPPFe(II)(OH). Accordingly, in cyclic voltammetry (Figure 1a), the reoxidation wave of the catalyst is located at ca. -1.10 V and corresponds to TPPFe(III)(OH)/TPPFe(II)(OH) couple (Figure S9). A small wave is also seen at ca. -1.75 V (Figure 1a). It can be attributed to the oxidation into TPPFe(II)(OH) of some TPPFe(I) accumulating in the diffusion-reaction layer, when the electrode potential gets more positive than the TPPFe(0)/TPPFe(I) standard potential. It is thus at variance with CO_2 electroreduction catalyzed by TPPFe(0) where the reoxidation wave corresponds to the TPPFe(I)/TPPFe(II) redox couple (Figure 1b). [25] Overall, the catalytic process taking place at -2.00 V corresponds to two intertwined catalytic cycles as sketched

in scheme 5.

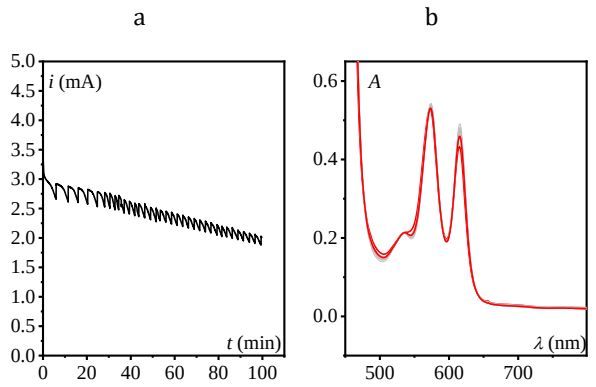

Figure 8. (a) Current over time upon electrolysis at -2.20 V after 100 min electrolysis at -1.80 V (Figure 7a) (b) Time evolution of UV-vis spectra (l = 1 mm, 1 scan / 75 s). Initial and final spectra in red.

Scheme 5. Electrochemical reduction of N_2O catalyzed by TPPFe(0)

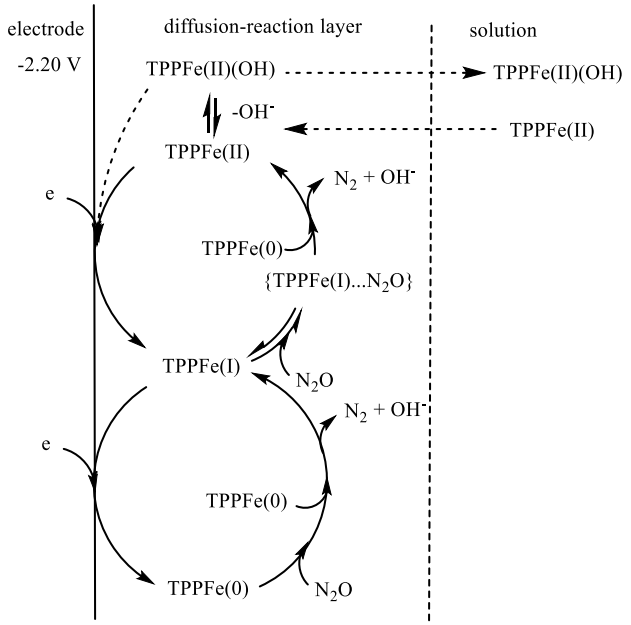

Conclusion

We have shown that the electroreduction of N_2O can be also catalyzed by TPPFe(I) albeit at a slower rate compared to TPPFe(0). This reactivity is at variance with the one of the isoelectronic CO_2 molecule, which does not react with TPPFe(I). The catalytic reduction of N_2O by TPPFe(I) is however endowed by a self-modulation process due to the production of hydroxide ions that bind to TPPFe(II) and slows down the regeneration of the active species TPPFe(I). Our results allow to rationalize the observation that the resting state in solution upon the electrocatalytic reduction of N_2O catalyzed by TPPFe(0) is TPPFe(II)(OH) and not TPPFe(I) as in the case of CO_2 catalytic reduction. An overall mechanism with two intertwined catalytic cycles is indeed taking place. Shifting the active catalysis from TPPFe(0) to TPPFe(I) opens the way toward the design of molecular catalytic systems for N_2O reductive deoxygenation at lower overpotential.

ASSOCIATED CONTENT

Supporting Information

Experimental details. Additional data.

ACKNOWLEGMENT

This work was supported by the Agence Nationale de la Recherche (DeNOSOr project ANR-22-CE07-0034-02), and Labex ARCANE (CBH-EUR-GS, ANR-17-EURE-0003). Ecole Normale Supérieure de Lyon is acknowledged for financial support for Camille Chartier. The MITI (Mission pour les Initiatives Transverses et Interdisciplinaires) program of the CNRS is gratefully acknowledged for Rana Deeba doctoral financial support. The NanoBio ICMG (UAR 2607) is acknowledged for providing facilities for NMR analyses. The authors thank Florian Molton for his technical assistance.

AUTHOR INFORMATION

Corresponding Authors

cyrille.costentin@univ-grenoble-alpes.fr

Notes

The author declares no competing financial interest.

REFERENCES

1. Zhang, W.; Lai, W.; Cao, R. Energy-Related Small Molecules Activation Reactions : Oxygen Reduction and Hydrogen and Oxygen Evolution Reactions Catalyzed by Porphyrin- and Corrole-Based Systems. *Chem. Rev.* **2017**, *117*, 3717-3797.

2. Boutin, E.; Merakeb, L. ; Ma, B. ; Boudy, B. ; Wang, M. ; Bonin, J. ; Anxolabéhère-Mallart, E. ; Robert, M. Molecular Catalysis of CO_2 Reduction : Recent Advances and Perspectives in electrochemical and Light-Driven Processes with Selected Fe, Ni and Co Aza Macrocyclic and Polypyridine Complexes. *Chem. Soc. Rev.* **2020**, *49*, 5772-5809.

3. Jin, S. ; Hao, Z. ; Zhang, K. ; Yan, Z.; Chen, J. Advances and Challenges for the Electrochemical Reduction of CO_2 to CO: From Fundamentals to Industrialization. *Angew. Chem. Int. Ed.* **2021**, *60*, 20627-20648.

4. Pauleta, S. R.; Carepo, M. S. P. ; Moura, I. Source and Reduction of Nitrous Oxide. *Coord. Chem. Rev.* **2019**, *387*, 436-449.

5. Severin, K. Synthetic Chemistry with Nitrous Oxide. *Chem. Soc. Rev.* **2015,** *44*, 6375-6386.

6. Deeba, R.; Molton, F.; Chardon-Noblat, S.; Costentin, C. Effective Homogeneous Catalysis of Electrochemical Reduction of Nitrous Oxide to Dinitrogen at Rhenium Carbonyl Catalysts. *ACS Catal.* **2021**, *11*, 6099-6103.

7. Costentin, C.; Robert, M.; Savéant, J-M. Current Issues in Molecular Catalysis Illustrated by Iron Porphyrins as Catalysts of the

CO2-to-CO Electrochemical Conversion. *Acc. Chem. Res.* **2015**, *48*, 2996-3006.

8. Stanley, J. S.; Wang, X. S.; Yang, J. Y. Selective Electrocatalytic Reduction of Nitrous Oxide to Dinitrogen with an Iron Porphyrin Complex. *ACS Catal.*, **2023**, *13*, 12617-12622.

9. Saito, S.; Ohtake, H.; Umezawa, N.; Kobayashi, Y.; Kato, N.; Hirobe, M.; Higuchi, T. Nitrous Oxide Reduction-coupled Alkene-alkene Coupling Catalysed by Metalloporphyrins. *Chem. Commun.*, **2013**, *49*, 8979-8981.

10. Bayachou, M.; Elkbir, L.; Farmer, P. J. Catalytic Two-Electron Reductions of N_2O and N_3^- by Myoglobin in Surfactant Films. *Inorg. Chem.*, **2000**, *39*, 289-293.

11. Amanullah, S.; Gotico, P.; Sircoglou, M.; Leibl, W.; Llansola-Portoles, M. J.; Tibiletti, T.; Quaranta, A.; Halime, Z.; Aukauloo, A. Second Coordination Sphere Effect Shifts CO_2 to CO Reduction by Iron Porphyrin from Fe^0 to Fe^I. *Angew. Chem. Int. Ed.* **2023**, e202314439.

12. Pugliese, E. ; Gotico, P.; Wehrung, I. ; Boitrel, B. ; Quaranta, A. ; Ha-Thi, M-H.; Pino, T.; Sircoglou, M.; Leibl, W.; Halime, Z.; Aukauloo, A. Dissection of Light-Induced Charge Accumulation at a Highly Active Iron Porphyrin: Insights in the Photocatalytic CO_2 Reduction. *Angew. Chem. Int. Ed.* **2022**, *61*, e202117530.

13. Amanullah, S.; Saha, P.; Dey, A. Activating the Fe(I) State of Iron Porphyrinoid with Second-Sphere Proton Transfer Residues for Selective Reduction of CO_2 to HCOOH via Fe(III/II)-COOH Intermediate(s). *J. Am. Chem. Soc.*, **2021**, *143*, 13579-13592.

14. Lexa, D.; Rentien, P.; Savéant, J-M.; Xu, F. Methods for investigating the mechanistic and kinetic role of ligand exchange reactions in coordination electrochemistry. Cyclic voltammetry of chloroiron(III)tetraphenylporphyrin in dimethylformamide. *J. Electronanal. Chem.* **1985**, *191*, 253-279.

15. Kosugi, K. ; Kondo, M. ; Masaoka, S. Quick and Easy Method to Dramatically Improve the Electrochemical CO_2 Reduction Activity of an Iron Porphyrin Complex. *Angew. Chem. Int. Ed.* **2021**, *60*, 22070-22074.

16. (a) It is however at variance with the observation of an adduct between TPPFe(I) and CO_2 by XAS-spectroscopy. (b) Mendoza, D.; Dong, S-T.; Kostopoulos, N.; Pinty, V.; Rivada-Wheelaghan, O.; Anxolabéhère-Mallart, E.; Robert, M.; Lassalle-Kaiser, B. *In situ* X-ray Absorption Spectroscopy in Homogeneous Conditions Reveals Interactions Between CO_2 and a Doubly and Triply Reduced Iron(III) Porphyrin, then Leading to Catalysis. *ChemCatChem*, **2022**, e202201298.

17. (a) DeSilva, C.; Czarnecki, K.; Ryan, M. D. Reaction of low-valent iron porphyrins with alkyl containing supporting electrolytes. *Inorg. Chim. Acta* **1994**, *226*, 195-201. (b) Mitchell, N. H.; Elgrishi, N. Investigation of Iron(III) Tetraphenylporphyrin as a Redox Flow Battery Anolyte: Unexpected Side Reactivity with the Electrolyte. *J. Phys. Chem. C*, **2023**, *127*, 10938-10946.

18. Salamé, A.; Cheah, M. H.; Bonin, J. ; Robert, M. ; Anxolabéhère-Mallart, E. Operando Spectroelectrochemistry Unravels the Mechanism of CO_2 Electrocatalytic Reduction by an Fe Porphyrin. *Angew. Chem. Int. Ed.*, **2024**, e202412417.

19. (a) In reference 19b, the spectrum attributed to TPPFe(0) in electrolysis experiments was wrongly attributed. It indeed corresponds to TPPFe(II)(*n*-Bu) (due to the reaction of TPPFe(0) with *n*-Bu_4N^+). TPPFe(II)(*n*-Bu) was the species that finally accumulated in the bulk when catalysis rate decreases in the absence of proton donor (b) Deeba, R.; Collard, A.; Rollin, C.; Molton, F.; Chardon-Noblat, S.; Costentin, C. Controlled Potential Electrolysis: Transition from Fast to Slow Regimes in Homogeneous Molecular Catalysis. Application to the Electroreduction of CO_2 Catalyzed by Iron Porphyrin. *ChemElectroChem*, **2023**, e202300350.

20. Balducci, G.; Chottard, G.; Gueutin, C. ; Lexa, D. ; Savéant, J-M. Electrochemistry of Iron(I) Porphyrins in the Presence of Carbon Monoxide. Comparison with Zinc Porphyrins. *Inorg. Chem.* **1994**, *33*, 1972-1978.

21. Römelt, C.; Song, J.; Tarrago, M.; Rees, J. A.; van Gastel, M.; Weyhermüller, T.; DeBeer, S.; Bill, E.; Neese, F.; Ye, S. Electronic Structure of a Formal Iron(0) Porphyrin Complex Relevant to CO_2 Reduction. *Inorg. Chem.* **2017**, *56*, 4745-4750.

22. Chartier, C.; Chardon-Noblat, S.; Costentin, C. Redox Behavior and Kinetics of Hydroxo Ligand Exchange on Iron Tetraphenylporphyrin: Comparison with Chloro Exchange and Consequences for its Role in Self-Modulation of Molecular Catalysis of Electrochemical Reactions. *Inorg. Chem.* **2024**, *63*, 7541-7548.

23. Costentin, C. Molecular Catalysis of Electrochemical Reactions. Overpotential and Turnover Frequency: Unidirectional and Bidirectional Systems. *ACS Catal.*, **2021**, *11*, 5678-5687.

24. Deeba, R.; Chardon-Noblat, S.; Costentin, C. Importance of Ligand Exchange in the Modulation of Molecular Catalysis: Mechanism of the Electrochemical Reduction of Nitrous Oxide with Rhenium Bipyridyl Carbonlyl Complexes. *ACS Catal.*, **2023**, *13*, 8262-8272.

25. (a) In the presence of a large amount of proton donor, catalysis is strong and the production of CO in the diffusion-reaction layer is large hence the reoxidation wave is shifted cathodically due to stabilization of TPPFe(II) via formation of TPPFe(II)(CO).[22b] (b) Costentin, C.; Drouet, S.; Passard, G. ; Robert, M. ; Savéant, J-M. Proton-Coupled Electron Transfer Cleavage of Heavy-Atom Bonds in Electrocatalytic Processes. Cleavage of a C-O Bond in the Catalyzed Electrochemical Reduction of CO_2. *J. Am. Chem. Soc.* **2013**, *135*, 9023-9031.

TOC

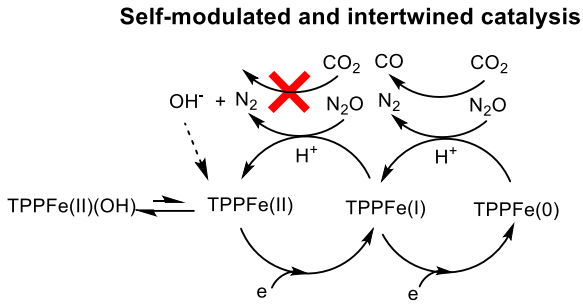
Self-modulated and intertwined catalysis
CO2
CO
CO2
OH- + N2
N2O
N2
N2O
H+
H+
TPPFe(II)(OH)
TPPFe(II)
TPPFe(I)
TPPFe(0)
e
e